nature plants

LETTERS

https://doi.org/10.1038/s41477-018-0316-5

The persistence of carbon in the African forest understory

Wannes Hubau[1,2,3,38]*, Tom De Mil[1,2,38], Jan Van den Bulcke[2,4], Oliver L. Phillips[3], Bhély Angoboy Ilondea[1,5,6], Joris Van Acker[2,4], Martin J. P. Sullivan[3], Laurent Nsenga[1], Benjamin Toirambe[1], Camille Couralet[1], Lindsay F. Banin[7], Serge K. Begne[3,8], Timothy R. Baker[3], Nils Bourland[1,9,10,11], Eric Chezeaux[12], Connie J. Clark[13], Murray Collins[14], James A. Comiskey[15,16], Aida Cuni-Sanchez[17,18], Victor Deklerck[2,4], Sofie Dierickx[1], Jean-Louis Doucet[10], Corneille E. N. Ewango[19,20,21], Ted R. Feldpausch[22], Martin Gilpin[3], Christelle Gonmadje[23], Jefferson S. Hall[24], David J. Harris[25], Olivier J. Hardy[26], Marie-Noel D. Kamdem[8,27], Emmanuel Kasongo Yakusu[1,2,21], Gabriela Lopez-Gonzalez[3], Jean-Remy Makana[19], Yadvinder Malhi[28], Faustin M. Mbayu[21], Sam Moore[28], Jacques Mukinzi[19,29], Georgia Pickavance[3], John R. Poulsen[13], Jan Reitsma[30], Mélissa Rousseau[1,11], Bonaventure Sonké[8], Terry Sunderland[9,31], Hermann Taedoumg[8], Joey Talbot[3], John Tshibamba Mukendi[1,21,32], Peter M. Umunay[33], Jason Vleminckx[26,34], Lee J. T. White[35,36,37], Lise Zemagho[8], Simon L. Lewis[3,17] and Hans Beeckman[1]

Quantifying carbon dynamics in forests is critical for understanding their role in long-term climate regulation[1–4]. Yet little is known about tree longevity in tropical forests[3,5–8], a factor that is vital for estimating carbon persistence[3,4]. Here we calculate mean carbon age (the period that carbon is fixed in trees[7]) in different strata of African tropical forests using (1) growth-ring records with a unique timestamp accurately demarcating 66 years of growth in one site and (2) measurements of diameter increments from the African Tropical Rainforest Observation Network (23 sites). We find that in spite of their much smaller size, in understory trees mean carbon age (74 years) is greater than in sub-canopy (54 years) and canopy (57 years) trees and similar to carbon age in emergent trees (66 years). The remarkable carbon longevity in the understory results from slow and aperiodic growth as an adaptation to limited resource availability[9–11]. Our analysis also reveals that while the understory represents a small share (11%) of the carbon stock[12,13], it contributes disproportionally to the forest carbon sink (20%). We conclude that accounting for the diversity of carbon age and carbon sequestration among different forest strata is critical for effective conservation management[14–16] and for accurate modelling of carbon cycling[4].

Investing in carbon storage and sequestration represent important strategies for climate change mitigation[3]. Forests have a potential to provide both long-lived carbon stocks[7,17] and long-term carbon sinks[1,2]. To successfully conserve forest carbon stock and

[1]Service of Wood Biology, Royal Museum for Central Africa, Tervuren, Belgium. [2]UGent-Woodlab, Laboratory of Wood Technology, Department of Environment, Ghent University, Ghent, Belgium. [3]School of Geography, University of Leeds, Leeds, UK. [4]Centre for X-ray Tomography , Ghent University, Ghent, Belgium. [5]Institut National pour l'Étude et la Recherche Agronomique, Kinshasa, Democratic Republic of the Congo. [6]École Régionale Postuniversitaire d'Aménagement et de Gestion intégrés des Forêts et Territoires tropicaux , Kinshasa, Democratic Republic of the Congo. [7]Centre for Ecology and Hydrology, Penicuik, UK. [8]Plant Systematic and Ecology Laboratory, Higher Teachers' Training College, University of Yaounde, Yaounde, Cameroon. [9]CIFOR, Bogor, Indonesia. [10]Forest Resources Management, Gembloux Agro-Bio Tech, University of Liège, Liège, Belgium. [11]Resources and Synergies Development, Singapore, Singapore. [12]Rougier-Gabon, Libreville, Gabon. [13]Nicholas School of the Environment, Duke University, Durham, NC, USA. [14]Grantham Research Institute on Climate Change and the Environment, London, UK. [15]Inventory and Monitoring Program, National Park Service, Fredericksburg, VA, USA. [16]Smithsonian Institution, Washington, DC, USA. [17]Department of Geography, University College London, London, UK. [18]Department of Geography and Environment, University of York, York, UK. [19]Wildlife Conservation Society-DR Congo, Kinshasa I, Democratic Republic of the Congo. [20]Centre de Formation et de Recherche en Conservation Forestière , Epulu, Democratic Republic of the Congo. [21]Faculté de Gestion de Ressources Naturelles Renouvelables, Université de Kisangani, Kisangani, Democratic Republic of the Congo. [22]Geography, College of Life and Environmental Sciences, University of Exeter, Exeter, UK. [23]National Herbarium, Yaounde, Cameroon. [24]ForestGEO, Smithsonian Tropical Research Institute, Panamá, Republic of Panama. [25]Royal Botanic Garden Edinburgh, Edinburgh, UK. [26]Service d'Évolution Biologique et écologie, Faculté des Sciences, Université Libre de Bruxelles, Brussels, Belgium. [27]Faculty of Science, Department of Botany and Plant Physiology, University of Buea, Buea, Cameroon. [28]Environmental Change Institute, School of Geography and the Environment, University of Oxford, Oxford, UK. [29]Salonga National Park, Kinshasa I, Democratic Republic of the Congo. [30]Bureau Waardenburg, Culemborg, the Netherlands. [31]Faculty of Forestry, University of British Columbia, Vancouver, Canada. [32]Faculté des Sciences Appliquées, Université de Mbujimayi, Mbujimayi, Democratic Republic of the Congo. [33]Yale School of Forestry and Environmental Studies, New Haven, CT, USA. [34]Department of Biological Sciences, Florida International University, Miami, FL, USA. [35]Agence Nationale des Parcs Nationaux, Libreville, Gabon. [36]Institut de Recherche en Écologie Tropicale, Libreville, Gabon. [37]School of Natural Sciences, University of Stirling, Stirling, UK. [38]These authors contributed equally: W. Hubau, T. De Mil. *e-mail: whubau@gmail.com

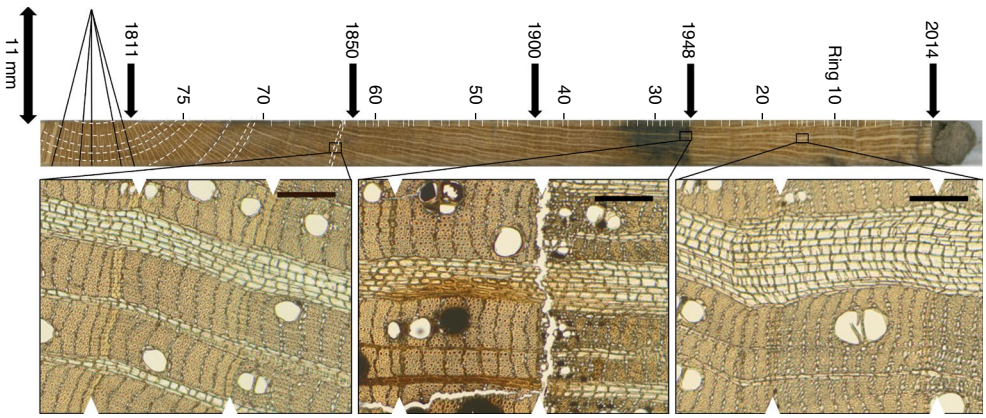

Fig. 1 | Example of a wood core (*Greenwayodendron suaveolens*, TreeID 765) showing the 1948 nail trace. The image at the top shows the full core. White lines indicate growth-ring boundaries, numbers indicate growth rings (counted from bark to pith), black arrows indicate important years. The bark to the right of the figure indicates the year of sampling (2014). The dark discoloration in growth rings 26 to 35 was caused by oxidates from the iron nail that were transported up and down in damaged vessels and fibres. The right border of the discoloration accurately marks the start of the year 1948. There are 25 rings between the bark and the 1948 nail trace, suggesting that this tree needed on average 2.6 years to form a ring. Using this rate for the 53 rings that were formed before 1948, we find that the first ring in the core was probably formed around 1811. The location of the pith is indicated by the black lines to the left, which follow the direction of the wood rays[41]. This shows that the distance from the pith to the first ring boundary in the core is about 11 mm. When using the average ring width of rings 78 to 68, we estimate that 7 rings are missing. Therefore, this tree would be about 224 years old. The three close-ups at the bottom illustrate wood anatomical details used to identify growth-ring boundaries (indicated by white triangles). Ring boundaries in this species are demarcated by distended wood rays and flattening of the fibres. Black scale bars, 0.2 mm.

increase forest carbon uptake, we must conserve carbon-rich forests and extend the forested land area[3] but decision makers and managers also need to understand the long-term behaviour of carbon within forests[1–3]. Critical questions are: (1) how long does the carbon persist and (2) where does it stay longest in the system? Carbon residence time is a direct function of tree longevity[3,7,17] but attempts to estimate tree age in tropical rainforests are relatively scarce and often highly contested[5–8]. Estimating the ages of the oldest trees in tropical forest stands is particularly subject to debate. While some authors claim that broadleaved trees in the tropics may reach ages of 1,000 years or older[8,18], others estimate maximum ages of not more than 600 years[5,6]. Furthermore, the oldest carbon in the system is often assumed to be located in large trees[8]. Canopy and emergent trees contain a large proportion of the stand-level biomass[12,14] but large trees alone may not represent the entire forest in terms of growth rates, tree lifespan and carbon persistence[7]. Canopy species grow faster[19] but there is a general trade-off between growth and lifespan in organisms[9,20]. Therefore, long-term carbon storage and sequestration in tropical rainforests may substantially depend on smaller trees too.

Here, we take advantage of a remarkable rediscovery of a historic forest inventory plot to probe the age structure of African rainforests in a way that has not been possible to date. The Nkulapark plot was established in 1948 in the southwest of the Democratic Republic of the Congo (Supplementary Fig. 1). A total of 6,315 trees with diameter at breast height (DBH) ≥5 cm were tagged and DBH was measured annually for 9 years. In 2014, we rediscovered and measured 450 surviving tagged trees, of which 55 were selected to measure growth ring series. We used the grown-in iron nail as a 1948 timestamp, giving accurate estimates of the DBH growth rate (mm yr^{-1}) and the rate of growth-ring formation (number of rings per year) over a 66 year period for each tree (Fig. 1 and Supplementary Table 1). The age of each tree (in years) was calculated as the total number of rings from pith to bark divided by the rate of growth-ring formation (number of rings per year) (Figs. 1 and 2). We used the five-class Crown Illumination Index of Dawkins and Field (hereafter CII)[21,22] to compare growth patterns and tree age among the different rainforest strata: understory (CII 1), sub-canopy (CII 2 and 3), canopy (CII 4) and emergent stratum (CII 5). Understory trees receive no direct light, sub-canopy trees receive lateral or restricted vertical light, canopy and emergent trees receive vertical light (Fig. 3a). Supplementary analyses show that the rediscovered Nkulapark tree dataset is adequate to compare age differences between forest strata (Supplementary Figs. 2 and 3; Supplementary Discussion).

We find that the age of the 55 Nkulapark trees with growth-ring series ranges between 129 and 452 years (Fig. 2 and Supplementary Table 1). There is no clear linear relationship between tree age and their DBH ($P=0.082$, Fig. 2a). Understory trees (CII 1) do not differ significantly in age from canopy and emergent trees (CII 4 or 5) ($P=0.254$, boxplot at the right of Fig. 2b), while trees in sub-canopy classes (CII 2 or 3) are slightly younger than trees in both the understory and the canopy. Despite their small size, understory trees (CII 1) can be surprisingly old. One *Microdesmis puberula* (TreeID 3,545) has an estimated age of 329 years with a DBH of just 156 mm (Supplementary Table 1).

To test if our findings hold true in a wider geographic context, we compared growth and age patterns among the different forest strata in 23 Central African permanent forest inventory plots[1,23] (Fig. 3, Table 1, Supplementary Fig. 1 and Supplementary Table 2). Selected plots had a similar species composition as in Nkulapark. Plots are demarcated rectangles or squares of median size 1 ha where each tree is mapped, tagged and measured according to standard protocols[1,2]. DBH of each tree with DBH ≥ 10 cm was measured at least twice. Small trees that grew larger than 10 cm during the monitoring period were recorded as recruits. Trees that died were recorded. We used repeated diameter measurements to estimate the growth rate of each tree. We estimated tree age by dividing the final diameter (mm) by the growth rate (mm yr^{-1}), assuming a constant growth rate over the lifetime of a tree[7]. We evaluated the robustness of this age estimation method using the rediscovered Nkulapark trees as a reference (Supplementary Fig. 4). Uncertainties are due to relatively short plot monitoring periods (average 9 years), yielding negative or zero growth rates for 9.7% of the trees. To avoid unrealistic tree age estimates, we replaced slow growth rates by a 'minimum allowed growth rate', defined as the x^{th} percentile of the growth rate distribution within each CII class. Sensitivity analysis showed that $x=25$ returned a realistic tree age distribution for our dataset (Supplementary Table 3; Supplementary Discussion). Further

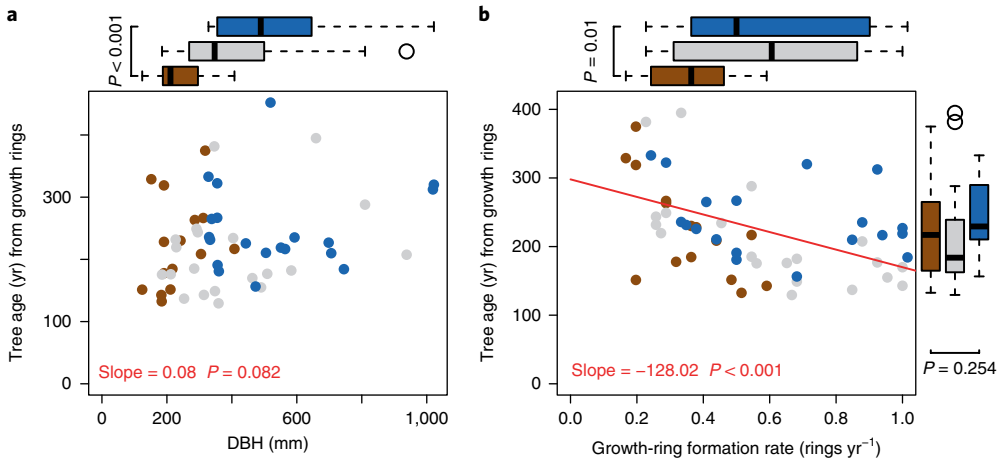

Fig. 2 | Variation in tree age inferred from growth-ring patterns in 55 trees where nail traces accurately mark the year 1948. a, The relationship between tree age and DBH. **b**, The relationship between tree age and the growth-ring formation rate (number of rings per year) between 1948 and 2014. In both panels, slopes and *P* values of simple linear regression models are given in red. Brown dots represent understory trees (Crown Illumination Index 1), grey dots represent sub-canopy trees (CII 2 and 3), blue dots represent canopy and emergent trees (CII 4 and 5) in 2014. Boxplots show the first quartile, the median value and the third quartile of the tree age distribution (vertical axis, boxplots to the right) and of the variables in the x-axis (horizontal boxplots at the top of the panels). *P* values under boxplots resulted from two-sided Wilcoxon rank-sum tests. Outliers are marked with open circles.

analysis suggests that x may be lower if monitoring periods are longer. Finally, we estimated tree-level mean carbon age as the average age of each year ring, weighted by the carbon content of the ring[7], with a year ring sequence deduced from the growth rate (see equation 2 in the Methods).

The mean tree age for the 23 plots across Central Africa ranged between 131 and 284 years, with an overall mean of 229 years (95% bootstrapped confidence intervals: 212–244 years) (Table 1). Mean tree age in the understory (CII 1) is estimated to be 262 years, which is significantly older than the overall mean ($P<0.001$) and older than the mean age of the sub-canopy (CII 3, 187 years, $P<0.001$), the canopy (CII 4, 194 years, $P<0.001$) and emergent classes (CII 5, 221 years, $P=0.021$) (Table 1). Furthermore, mean carbon age at the tree level is 65 years (95% confidence interval 61–70). Carbon stored in the understory trees (CII 1) is estimated to be on average 74 years (69–79), which is significantly older than the overall mean ($P<0.001$) and older than carbon stored in the sub-canopy (CII 3, 54 years, $P<0.001$) and the canopy (CII 4, 57 years, $P=0.001$). However, the difference between mean carbon age in the understory (CII 1) versus the emergent class (CII 5, 66 years) is not significant ($P=0.086$) (Fig. 3b and Table 1).

For each plot, we calculated the contribution of each forest stratum (in %) to the total above-ground biomass-carbon stock (AGC-stock) and to the total AGC-sink using standard methods[1,2] (Table 1). The AGC-stock (in Mg C ha^{-1}) represents the carbon reservoir in the system while the AGC-sink (in Mg C ha^{-1} yr^{-1}) represents the net change, calculated as AGC-productivity (additions to the system from tree growth) minus AGC-mortality (losses)[17]. The understory (CII 1) contributes 11% to the total plot-level AGC-stock (Table 1) and 20% to the plot-level AGC-sink. In contrast, the sub-canopy classes (CII 2 and 3) together contribute about 25% to the AGC-stock, but nothing to the AGC-sink. The understory thus contributes disproportionally to carbon sequestration, considering its relatively small share in the stock and compared to the limited contribution of the sub-canopy classes.

Discussion

Results from both the Nkulapark dataset (Fig. 2) and the 23 inventory plots (Fig. 3; Table 1) show that understory (CII 1) and emergent (CII 5) trees are on average older than sub-canopy trees (CII 3). This pattern can be explained by differences in life-history strategies[15]. Understory specialist species maintain low growth rates for long periods, resulting in relatively small DBH at older age. Their adaptations allow them to survive in the understory without the need to invest in rapid growth. The sub-canopy classes (CII 2 and 3) are dominated by suppressed canopy specialists that survived a recruitment stage but did not reach the canopy yet. These trees are relatively young (Fig. 3) and they experience limited light conditions, resulting in mortality rates equal to productivity rates. Canopy and emergent trees (CII 4 and 5 respectively) are canopy specialists that have been able to grow rapidly for long periods[24]. This is in line with previous work[19] showing that growth rates in emergent trees are high and increase continuously. To test the assumption that high tree and carbon age in the understory may be due to a difference in species composition, we classified species as (1) understory specialists, (2) non-specialists and (3) canopy specialists (Supplementary Discussion). This confirmed that understory specialists are on average smaller ($P<0.001$) but older ($P<0.001$) than canopy specialists (Supplementary Table 4).

Furthermore, the Nkulapark dataset shows that there is a significant negative relationship between tree age and growth-ring formation rate (Fig. 2b). Of the trees in the dataset, 91% did not form a growth ring every year, indicating an aperiodic growth pattern (shifts of growth to dormancy and back do not occur annually). This aperiodic growth pattern is more prominent in understory trees, which formed fewer growth rings (0.36 rings per year) than canopy and emergent trees (0.61 rings per year) ($P=0.01$; boxplots at the top of Fig. 2b). Aperiodic growth patterns translate into significantly slower long-term growth rates: understory trees (CII 1) have a mean DBH growth rate of 1.51 mm yr^{-1} versus 4.99 mm yr^{-1} in emergent trees ($P<0.001$) (Table 1). The observed differences in growth periodicity (Fig. 2b), growth rates (Table 1) and age distribution (Fig. 3) among the different forest strata are most likely a result of differences in survival mechanisms which are a function of resource availability[11,25,26] (Supplementary Discussion).

Our data show that growth and age distribution of tropical trees in mixed lowland rainforests is complex. Large canopy trees are among the oldest in the rainforest, as suggested by several authors[8] but as they obtained their size and position by maintaining fast growth rates[19], they are not significantly older than slow-growing small understory specialists (Figs. 2 and 3 and Table 1). Furthermore, while large canopy trees represent the largest share of

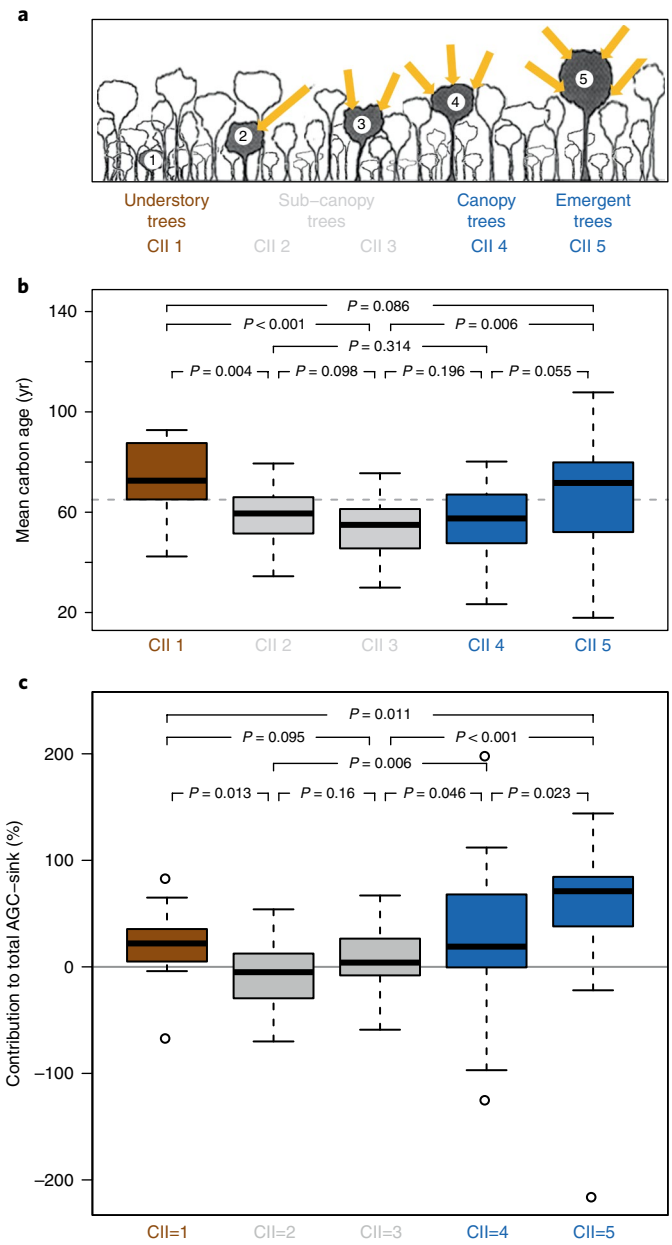

Fig. 3 | Estimation of mean carbon age and contribution to above-ground carbon (AGC) sink per crown illumination category for 23 permanent inventory plots in Central Africa. The 450 rediscovered Nkulapark trees were treated as an additional plot to estimate distributions of mean carbon age. **a**, The Crown Illumination Index (CII) developed by Dawkins and Field[22], with yellow arrows indicating reception of sunlight (drawing modified from ref. [21]). Understory trees (brown; CII 1) receive no direct sunlight, sub-canopy trees (grey) receive lateral (CII 2) or restricted vertical (CII 3) light, canopy trees (blue; CII 4) are almost completely exposed to vertical light and emergent trees (blue; CII 5) have a crown that is completely exposed to vertical and lateral light. **b**,**c**, Boxplots show the distribution of plot-level mean carbon age and the contribution to the total plot-level AGC-sink per CII class. Boxplots represent the 25% quartile, the median value and the 75% quartile of the plot-level average ages. Outliers are marked with open circles. Comparison among CII classes was performed with Dunn's rank-sum test using the Benjamini–Hochberg adjustment for multiple comparisons[50]. The grey dotted line shows the overall (plot-level) average age.

the carbon stock[12–14], they suffer most during droughts[27]. In comparison, understory trees represent a smaller carbon capital but are less vulnerable to drought and contribute disproportionately to carbon sequestration. As such, the understory provides long-term stability in forest carbon cycling. Furthermore, the understory is more diverse than the canopy in terms of species composition[14–16]. Therefore, we recommend quantifying forest ecosystem services by considering forests as a whole, with all forest strata providing specific services[16]. This is important in Central Africa, where the demand for fuelwood and charcoal could severely affect the understory if only large trees were to be protected[14,28].

Finally, our results suggest that care is required with large-scale modelling of forest carbon accumulation potential and responses to different climate change scenarios[4]. There are two hypothesized responses to increasing atmospheric CO_2 concentrations, possibly explaining the observed long-term AGC-sink in tropical forests[1,2]: (1) big trees increasing their asymmetric competition to the detriment of the rest of the stand or (2) suppressed trees do best, as they are closer to their light compensation point[17,29]. Our results show that both scenarios occur in forest stands, with the understory (CII 1), the canopy (CII 4) and the emergent (CII 5) classes contributing to carbon sequestration, while the sub-canopy classes (CII 2 and 3) do not contribute. Forest and carbon cycle models will need to account for the diversity of carbon age and carbon sequestration potential among the different forest strata. Recent studies have found that forest structure can be predicted from the characteristics of canopy trees[13,14] but our results suggest that temporal dynamics differ between forest strata. The long-term persistence of function depends on smaller trees too, which compared to their stature contribute disproportionately more to long-term carbon storage, sequestration and climate resilience.

Methods

Site description. The Nkulapark is a phenology and tree-growth monitoring plot covering 174 ha within the Luki Man and Biosphere reserve, located in the southern Mayumbe mountains in the Democratic Republic of the Congo[25] (Supplementary Fig. 1). The region is situated around 13.10°E and 5.62°S and experiences a humid tropical climate with a dry season between mid-May and mid-October and a short dry season from mid-December to mid-February. Yearly precipitation ranges from 649 mm to 1,853 mm with a mean precipitation of 1,173 mm. Temperature ranges between 19 °C and 30 °C with a mean temperature of 25.5 °C (ref. [25]). The Nkulapark is situated almost entirely in a catchment with a valley and a ridge and includes several microclimatic conditions. The semideciduous lowland forest consists of (1) mature forest dominated by *Prioria balsamifera*, (2) old regenerating forest dominated by *Terminalia superba*, (3) mixed-species mature forest and (4) modified forest patches[30,31].

Nkulapark plot design in 1948. The Nkulapark was established and managed by the Institut National pour l'Étude Agronomique du Congo Belge (INEAC), later renamed Institut National pour l'Étude et la Recherche Agronomique en R.D.Congo (INERA, http://www.inera-drc.org). In charge of the tagging and the measurements was Léon Toussaint who worked as a botanist in the Luki reserve between 1946 and 1952 (ref. [32]). The planning of the plot was first announced in the INEAC–Luki annual report of 1946 (ref. [33]). A total of 29.2 km of observation paths were cut in the forest in 1947, following the contour lines of the Nkula river valley (Supplementary Fig. 1)[30]. A total 6,315 trees were tagged by the end of 1947 (ref. [30]), so we assume that first wood formation after tagging occurred during the wet season that started in October 1948. Tree selection was performed by randomly selecting trees from the pool of trees >5 cm DBH in 1948. The Nkulapark area was mapped, showing the locations of the largest tagged trees. From 1948 to 1957 yearly diameter measurements were performed on all tagged trees[34]. Mortality events were recorded in the datasheets. Trees were measured at a height of 1.3 m and the point of measurement (POM) was indicated on the tree with a horizontal line of lead-based paint. For trees with buttresses or deformities, the POM was raised to a point high enough to avoid the irregularities interfering with diameter measurements at subsequent censuses. For trees with extremely high buttresses, diameters were estimated. For the same 6,315 trees, weekly phenology observations were recorded. Phenological observations were done for leaf habit, flowering, fruiting and seed dissemination. The plot was abandoned in 1957 but the datasheets were kept in the library of the INERA station in Luki and digitized in 2008 (ref. [25]) and 2014.

Table 1 | Estimation of tree age, mean carbon age, contribution to total above-ground carbon sink (AGC-sink), contribution to total AGC-stock and leaf habit per crown illumination category for 23 permanent forest plots

metric	All trees	CII 1	CII 2	CII 3	CII 4	CII 5	*P* value
Tree age (yr)	229 (212–244)	262 (243–282)	210 (196–223)	187 (170–204)	194 (175–212)	221 (192–250)	0.021
Mean carbon age (yr)	65 (61–70)	74 (69–79)	60 (55–64)	54 (49–59)	57 (51–63)	66 (57–75)	0.086
Contribution to total AGC-sink (%)	100	20 (9–32)	−8 (−21–5)	7 (−5–19)	28 (0–56)	52 (22–76)	0.011
Contribution to total AGC-stock (%)	100	11 (8–14)	15 (12–18)	10 (7–13)	31 (25–39)	33 (27–39)	<0.001
Stem density (stems ha^{-1})	428 (392–465)	194 (165–228)	112 (94–130)	38 (33–44)	59 (46–70)	25 (19–31)	<0.001
DBH (mm)	313 (291–338)	161 (154–168)	235 (222–250)	299 (273–326)	435 (397–469)	700 (644–760)	<0.001
DBH growth (mm yr^{-1})	2.38 (2.17–2.63)	1.51 (1.35–1.69)	2.16 (1.96–2.38)	2.98 (2.69–3.31)	4.03 (3.71–4.34)	4.99 (4.32–5.68)	<0.001
Wood density (g cm^{-3})	0.59 (0.56–0.61)	0.64 (0.62–0.65)	0.61 (0.6–0.63)	0.59 (0.56–0.61)	0.59 (0.56–0.61)	0.57 (0.53–0.61)	0.006
Ratio evergreen/ deciduous	3.27 (2.85–3.71)	4.72 (3.86–5.59)	4.61 (2.76–7.85)	3.62 (2.78–4.6)	3.03 (2.09–4.22)	1.78 (0.88–3.43)	<0.001
Proportion evergreen trees (%)	55 (52–57)	56 (52–59)	55 (51–59)	56 (52–61)	51 (46–56)	44 (37–52)	0.01
Proportion deciduous trees (%)	18 (16–20)	14 (12–17)	19 (16–22)	21 (17–25)	26 (21–31)	35 (28–41)	<0.001

The 450 rediscovered Nkulapark trees were treated as an additional plot for estimation of tree age and mean carbon age (first two rows). All metrics were averaged per plot and per CII class. Reported values are means , 95% confidence intervals are given between brackets. Components of AGC-stock are diameter (DBH), wood density and stem density. Comparison among CII classes was performed with Dunn's rank-sum test using the Benjamini–Hochberg adjustment for multiple comparisons[50]; the reported *P* values compare CII 1 and CII 5.

Rediscovering Nkulapark trees in 2014. Each of the original 6,315 Nkulapark trees were labelled during the first census in 1948 with a zinc number tag attached to the tree using an iron nail of 8 cm long. Some of these trees were indicated on the original 1948 map. During a first prospective field campaign in August 2014, this map was digitized and georeferenced with QGIS (QGIS development team, 2016) using landmarks such as easily rediscovered trees, contour lines and observation paths that were still visible and could be tracked with a Garmin 64s GPSmap (Supplementary Fig. 1). Based on this map, we pinpointed the approximate location of 1,521 trees that were recorded as alive during the last census in 1957. During a second field campaign in September–October 2014, these 1,521 trees were searched for: 450 were found alive, 16 were dead and the remaining 1,057 could not be relocated and were assumed to be dead and rotted away, albeit some may have been missed (Supplementary Figs. 2 and 3; see Supplementary Discussion for an indepth analysis of survivorship rates). The original 1948 tree tags and nails of the rediscovered trees were either still present outside the trunk or detected inside the tree using a metal detector (BHJS, Bounty Hunter). Scars on the trunk indicated the presence of an overgrown nail and repelled number tags were sometimes found on or in the ground nearby the tree using the metal detector. In most cases, the numbers on the tags were still readable. On 95% of the rediscovered trees, the lead-based paint of the POM was still visible, allowing a representative DBH measurement. Comparison of DBH, DBH growth rates and tree age distribution in the original dataset of Nkulapark trees versus the dataset of rediscovered trees, showed that the rediscovered dataset is slightly biased towards discovering slower-growing trees but this bias affected both classes of understory and canopy specialist species (Supplementary Fig. 3). Hence, the rediscovered tree dataset is representative to compare growth and age patterns among the different forest strata in the Nkulapark area.

Sampling Nkulapark trees in 2014. Wood samples for growth-ring analysis were taken from rediscovered trees if the following criteria were met: (1) the nail was still present in the wood, either totally grown-in or partly sticking out of the trunk, (2) the exact position of the nail could be identified visually or with the metal detector, (3) the nail was not overgrown by excessive wound tissue, buttresses or other deformities. As such, increment cores or stem discs were taken near the nail for 58 of the rediscovered trees. For each sampled tree, increment cores were taken a few centimetres above, below, to the left and to the right of the nail using a 40 cm Pressler bore. For each tree, two additional cores were taken at 120° from the nail trace along the circumference of the tree. As such, six increment cores were available for each tree. This maximized the chance of sampling the pith of the tree. To study and describe the reaction of the wood after tagging, additional larger wood samples containing the nail were extracted from 30 trees using a saw and a chisel.

Visualizing and measuring growth-ring series. For each wood core, growth-ring series were visualized using two imaging methods as previously described[35]: (1) first, density profiles were calculated from X-ray computed tomography scans of entire wood cores, then (2) the cores were surfaced with a core microtome[36] and scanned using a flatbed scanner (EPSON Perfection 4990 PHOTO). To obtain X-ray computed tomography volumes, cores were scanned at 110 µm resolution with the Nanowood computed tomography facility from the Centre for X-ray Computed Tomography of Ghent University (UGCT, www.ugct.ugent.be)[37], developed in collaboration with XRE (www.xre.be; now part of the TESCAN ORSAY HOLDING a.s.). Reconstruction was performed with the Octopus software package on a GeForce GPX 770 4 GB GPU (refs [37,38]). X-ray and flatbed scans were analysed using the toolchain for tree-ring analysis described by De Mil et al.[35]. This toolchain semi-automatically indicates the growth-ring boundaries and calculates growth-ring width series. Depending on the visibility of the growth-ring patterns, either the X-ray or the flatbed scans were used to check growth-ring boundaries and measure growth-ring widths. Growth-ring boundaries were distinguished using visual wood anatomical characteristics such as distended rays, flattened fibres and terminal parenchyma bands[5,39,40]. For unclear ring boundaries, microscopic thin sections were taken to study wood anatomy at high resolution using an Olympus BX60 microscope (Fig. 1).

Detecting the 1948 nail trace. Discolorations or wound tissue formed as a reaction on the tagging were visible in the cores taken near the nail. The surface of these stem discs was sanded to a few millimetres above the nail and the anatomy was observed using an Olympus BX60 microscope. The nails were remarkably well preserved inside the trees, probably due to cathodic protection of the iron by the zinc of the tags. Hence, discolorations or wound tissue were visible in each of these samples. Discolorations were recognizable as darkened tissue in otherwise light-coloured wood (Fig. 1). Discolorations occurred in cells that were formed before the nail was inserted due to oxidation processes between the wood and the iron nail. Water in vessels and fibres near the nail (especially those damaged by the nail) spread these oxidates upwards and downwards. Therefore, the discolorations in these cells are also detectable on samples taken a few centimetres under or above the nails. Vessels and fibres formed after the tagging were not damaged, hence did not show discolorations. As such, the boundary of the discoloration accurately serves as a timestamp indicating the year of tagging (1948). Furthermore, wound-induced deformities occurred in the wood that was formed after the nail was inserted. This wound tissue is characterized by increased woody productivity around the nail, forming a lump in the growth rings formed just after the nail was inserted. This lump formation is not present in the wood that was formed before tagging.

Estimating tree age using growth rings and nail traces. Six cores were assessed for each tree. For some trees, none of the cores contained the pith because (1) the tree radius exceeded the borer length or (2) the pith was eccentric and missed. In these cases, the core with the largest number of visible rings was used to estimate the total number of growth rings. The missing core length from the end of this core

to the pith was estimated using the intersection of three lines of ring boundaries marked along the rays, as described by Hietz[41] (see Fig. 1 for an example). We estimated the number of rings in the missing core part by dividing the missing core length by the average ring width of the five oldest rings of the sampled core. We tested the robustness of this method by re-running the analysis using the average growth rates of the 5, 10, 15 and 20 oldest rings. We found that the overall average tree age and the trends observed in Fig. 2 are not sensitive to varying the method used to estimate the number of rings in the missing part of the core. The core with the clearest nail trace was used to count the number of rings formed after the year of tagging (1948). We used the number of growth rings formed between 1948 (nail mark) and 2014 (cambium) as a reference to calculate the number of years the tree needed to form one ring (years per ring). We then multiplied this ratio with the total number of rings formed before 1948 to estimate the age of the tree (Figs. 1 and 2). Three trees were not used for analysis because the estimated missing core length of each core exceeded 20 cm. As such, growth-ring series of 55 trees were retained (Supplementary Table 1).

Permanent forest inventory plots. To test if our findings hold true in a wider geographic context, we estimated mean tree age and carbon age of the different forest strata using plots from the African Tropical Rainforest Observation Network (AfriTRON; www.afritron.org). We selected 23 permanent forest plots located in four different Central African countries (Cameroon, Gabon, Congo Brazzaville, D.R.Congo) (Supplementary Fig. 1 and Supplementary Table 2)[23]. Plots were selected if at least 65% of the trees belonged to species that also occur in Nkulapark. Furthermore, plots selected for analysis conformed to the following criteria[1,2,23]: (1) plots had an actual plot area of ≥0.2 ha, (2) plots were georeferenced, (3) all trees with DBH ≥ 100 mm were measured, (4) the majority of stems were identified to species level, (5) plots had at least two censuses, (6) plots had a total monitoring length of ≥3 yr, (7) plots were situated within structurally intact, apparently mature forest (excluding young or open forests), (8) plots were free from major human impacts, (9) plots were located at ≥50 m from the anthropogenic forest edge, (10) altitude was below 1,500 metres above sea level, (11) mean annual air temperature was ≥20.0 °C, (12) mean annual precipitation was ≥1,000 mm yr^{-1}, (13) plots were located in terra firme forest and (14) the CI index was recorded for each tree in the plot. For analysis purposes, plots smaller than 0.5 ha that were within 1 km of each other and located in similar forest types were merged (that is the LME cluster). AfriTRON plot data are curated in the ForestPlots.net database[42] and subject to identical quality control and quality assurance procedures. All calculations of plot data metrics described hereafter were performed using the R statistical platform[43], version 3.2.1.

Estimating AGC-stock. For each tree and each census, above-ground Biomass at the tree level (AGB, Mg $stem^{-1}$) was estimated using a published allometric equation for moist forests including terms for diameter (DBH, mm), dry wood density (ρ, g cm^{-3}) and total tree height (H, m)[44]:

$$\mathrm{AGB} = \frac{0.0673 \times \left(\rho \times \left(\frac{\mathrm{DBH}}{10}\right)^2 \times H\right)^{0.976}}{1,000} \quad (1)$$

Wood density values were derived from the dryad database (www.datadryad.org). Stems were matched to species-specific wood density values or the mean values for the genus or family[1,42]. Heights were calculated using a single height-diameter model (Weibull) for central African lowland terra firme forests[45], using commands implemented in the R-package BiomasaFP(ref. [46]). Above-ground Biomass-Carbon (referred to as AGC) is considered as 47% of the AGB following IPCC recommendations[47]. For each tree in the plot dataset, AGC-stock was calculated as the mean of the first and last censuses. Finally, we calculated the AGC-stock in each CII class in each plot, divided by the total plot-level AGC-stock and multiplied by 100 to express the results as % of the total plot-level AGC-stock.

Estimating AGC-sink. For the calculation of AGC-sink, only the first and the last censuses were used for each plot. First, AGC- productivity (Mg C $stem^{-1}$ yr^{-1}) for each stem surviving the monitoring period, was calculated as the difference between its total AGC at the end census minus the total AGC at the start census of the interval, divided by the census interval length (yr). AGC-productivity for stems recruited during the monitoring period (that is reaching DBH ≥ 100 mm), was calculated in the same way, assuming DBH to be 0 mm at the start of the interval. AGC-mortality for each tree that died during the monitoring period (Mg C $stem^{-1}$ yr^{-1}) was calculated as the AGC at the start of the monitoring period, divided by the total monitoring length (yr). AGC-productivity at the stand level (Mg C ha^{-1} yr^{-1}) was then calculated as the sum of tree-level productivity estimates of all survivors and recruits. AGC-mortality at the stand level (Mg C ha^{-1} yr^{-1}) was calculated as the sum of tree-level mortality estimates of all dead trees in the subset. We corrected for unobserved components of biomass growth and mortality due to census interval length effects[2,48,49]. A method to correct productivity and mortality rates for these uncertainties was developed by Talbot et al.[48]. This correction accounts for (1) trees that recruit and die within the same interval (unobserved recruits) and (2) growth of trees that grow and die within the interval (unobserved biomass growth from mortality, which is not recorded because dead trees are not measured). For each census interval, we calculated unobserved recruitment and unobserved mortality components (Mg ha^{-1} yr^{-1}) using the formulas proposed by Talbot et al.[48] and both components were added to both the AGC-productivity and AGC-mortality estimates. Estimates of the unobserved biomass components usually accounted for less than 3% of the total AGC-productivity and AGC-mortality. The AGC-sink was calculated as stand-level AGC-productivity minus AGC-mortality. Finally, we calculated the AGC-sink for each CII class in each plot, divided by the total plot-level AGC-sink and multiplied by 100 to express the results as % of the total plot-level AGC-sink. Absolute sink values are not reported because the total sink is likely to be overestimated due to a relatively small sample size (23 plots), possibly capturing occasional natural disturbance events. Commands to calculate AGC-stock and AGC-sink are implemented in the BiomasaFP R-package[46].

Tree age inferred from DBH growth rates in permanent inventory plots. For each tree within the permanent forest inventory plots, we estimated the age by dividing the DBH (mm) in the final census by the DBH growth rate (mm yr^{-1}) of the tree itself. For each tree, we averaged the DBH growth rate over all census intervals preceding the last census. This method uses the actual growth rate of each tree, which is accurate for healthy trees but returns unrealistic age estimates for trees with (1) slightly negative growth rates, (2) zero growth rates or (3) very slow growth rates. Such slow growth rates may be recorded in all DBH classes. First, slow growth rates in large DBH classes may occur when a tree is diseased or at the end of its life (senescence). These growth rates may not be representative for the total lifespan of these trees. Secondly, small growth rates may be recorded for small suppressed trees if their growth is so slow that it cannot be recorded with sufficient precision using standard census procedures. Hence, these growth rates are replaced by growth rates that yield a realistic tree age estimate. As such, we chose a 'minimum allowed growth rate' per CII class, following Vieira et al.[7]. We calculated the minimum allowed growth rate for each CII class as the 25th percentile (first quartile) of the growth rate distribution within the CII class. For each tree with a growth rate slower than the minimum allowed rate, we replaced the growth rate by the minimum allowed growth rate of the CII class. We conducted a sensitivity analysis to check how results vary when varying the minimum allowed growth rate: we re-ran the analysis using the 10th, 15th, 20th, 25th and 30th percentile of the growth rate distribution within each CII class as a minimum allowed growth rate (Supplementary Discussion and Supplementary Table 3). We used the average tree age in the dataset of 450 rediscovered Nkulapark trees as a reference to evaluate the tree-age estimation method based on DBH growth rates (Supplementary Fig. 4).

Mean carbon age. As a tree grows, it increasingly stores more carbon. Carbon in growth-rings near the bark of the tree is younger than carbon in the pith. Because of this, mean carbon age of a tree does not equal total tree age. For each tree in the selected 23 plots, we deduced a year-ring series using its final DBH and the DBH growth rate (mm yr^{-1}), assuming a constant growth rate over the lifetime of the tree. We then used this deduced year-ring series to calculate mean tree-level carbon age using the same formula as Vieira et al.[7]:

$$\text{mean carbon age} = \frac{\sum_{i=1}^{n} (C_i \times A_i)}{\sum_{i=1}^{n} (C_i)} \quad (2)$$

with C_i the carbon content of the ith ring (kg), A_i is the age of the ith ring (yr) and n is the number of rings.

The carbon content of the ith ring is calculated as the carbon content of a tree with the DBH of ring i minus the carbon content of a tree with the DBH of ring $i-1$.

Classification of tree species and statistical analysis. To distinguish between understory, sub-canopy, canopy and emergent trees in the Nkulapark and in the 23 permanent forest plots, we used the Crown Illumination Index (CII) of Dawkins and Field[22]. Figure 3 illustrates the five classes with a drawing modified from Synnott[21]. In each plot, each tree was attributed to one of the CII classes. The index was attributed in the field, mostly during one census and mostly by a single person. We estimated mean tree age, mean carbon age, mean AGC-stock and mean AGC-sink for each of the CII classes in each plot. None of the metrics reported in Table 1 meets the criterion of homogeneity of variances (Bartlett test). Therefore, differences among the CII classes were tested using the non-parametric Dunn's rank-sum test. To avoid the multiple comparison problem, we used the Benjamini–Hochberg P value adjustment[50] ('dunn.test' package in R, ref. [43]).

Reporting Summary. Further information on research design is available in the Nature Research Reporting Summary linked to this article.

Data availability

The input data and R-scripts to generate the figures and tables are available for download using the following private link: https://figshare.com/

s/06c793575d3b52ef5574. Images of wood cores are available using the following link: https://figshare.com/s/e6101fe7d330f8ea140a. This folder also contains all annotation documents needed to visualize growth ring boundaries on the wood samples (please consult the README document for guidelines). Wood samples used to conduct this analysis are stored in the Tervuren xylarium (http://www.africamuseum.be/collections/browsecollections/naturalsciences/earth/xylarium). These samples may be studied, within the Tervuren xylarium, on request addressed to the curator H.B. (hans.beeckman@africamuseum.be) or the corresponding author W.H. (whubau@gmail.com).

Received: 11 May 2018; Accepted: 30 October 2018;
Published online: 21 January 2019

References

1. Lewis, S. L. et al. Increasing carbon storage in intact African tropical forests. *Nature* **457**, 1003–1006 (2009).
2. Brienen, R. J. W. et al. Long-term decline of the Amazon carbon sink. *Nature* **519**, 344–348 (2015).
3. Körner, C. A matter of tree longevity. *Science* **355**, 130–131 (2017).
4. Galbraith, D. et al. Residence times of woody biomass in tropical forests. *Plant Ecol. Divers.* **6**, 139–157 (2013).
5. Brienen, R. J. W., Schöngart, J. & Zuidema, P. A. in *Tropical Tree Physiology* Vol. 6 (eds. Goldstein, G. & Santiago, L. S.) 439–461 (Springer, New York, 2016).
6. Worbes, M. One hundred years of tree-ring research in the tropics – a brief history and an outlook to future challenges. *Dendrochronologia* **20**, 217–231 (2002).
7. Vieira, S. et al. Slow growth rates of Amazonian trees: consequences for carbon cycling. *Proc. Natl Acad. Sci. USA* **102**, 18502–18507 (2005).
8. Chambers, J. Q., Higuchi, N. & Schimel, J. P. Ancient trees in amazonia. *Nature* **391**, 135–136 (1998).
9. Bigler, C. Trade-offs between growth rate, tree size and lifespan of mountain pine (*Pinus montana*) in the Swiss national park. *PLoS ONE* **11**, 1–18 (2016).
10. Kleczewski, N. M., Herms, D. A. & Bonello, P. Effects of soil type, fertilization and drought on carbon allocation to root growth and partitioning between secondary metabolism and ectomycorrhizae of *Betula papyrifera*. *Tree Physiol.* **30**, 807–817 (2010).
11. Sass-Klaassen, U. Tree physiology: tracking tree carbon gain. *Nat. Plants* **1**, 15175 (2015).
12. Bastin, J.-F. et al. Seeing Central African forests through their largest trees. *Sci. Rep.* **5**, 1–8 (2015).
13. Bastin, J. -F. et al. Pan-tropical prediction of forest structure from the largest trees. *Glob. Ecol. Biogeogr.* **27**, 1366–1383 (2018).
14. Lutz, J. A. et al. Global importance of large-diameter trees. *Glob. Ecol. Biogeogr.* **27**, 849–864 (2018).
15. Memiaghe, H. R., Lutz, J. A., Korte, L., Alonso, A. & Kenfack, D. Ecological importance of small-diameter trees to the structure, diversity and biomass of a tropical evergreen forest at Rabi, Gabon. *PLoS ONE* **11**, 1–15 (2016).
16. Burton, J. I., Ares, A., Olson, D. H. & Puettmann, K. J. Management trade-off between aboveground carbon storage and understory plant species richness in temperate forests. *Ecol. Appl.* **23**, 1297–1310 (2013).
17. Lloyd, J. & Farquhar, G. D. The CO_2 dependence of photosynthesis, plant growth responses to elevated atmospheric CO_2 concentrations and their interaction with soil nutrient status. I. General principles and foreste cosystems. *Funct. Ecol.* **10**, 4–32 (1996).
18. Laurance, W. F. et al. Inferred longevity of Amazonian rainforest trees based on a long-term demographic study. *Forest Ecol. Manag.* **190**, 131–143 (2004).
19. Stephenson, N. L. et al. Rate of tree carbon accumulation increases continuously with tree size. *Nature* **507**, 90–93 (2014).
20. Wright, S. J. et al. Functional traits and the growth — mortality trade-off in tropical trees. *Ecology* **91**, 3664–3674 (2013).
21. Synnott, T. J. *A Manual of Permanent Plot Procedures for Tropical Rain Forests* Tropical Forestry Papers No. 14 (Department of Forestry Commonwealth Forestry Institute, Oxford Univ., 1979).
22. Dawkins, H. C. & Field, D. R. B. *A Long-term Surveillance System for British Woodland Vegetation* C.F.I. Occasional Papers 1 (Oxford Univ., 1978).
23. Lewis, S. L. et al. Above-ground biomass and structure of 260 African tropical forests. *Philos. Trans. R. Soc. B* **368**, 20120295 (2013).
24. Hall, J. S., Harris, D. J., Medjibe, V. P. & Ashton, M. S. The effects of selective logging on forest structure and tree species composition in a Central African forest: implications for management of conservation areas. *Forest Ecol. Manage.* **183**, 249–264 (2003).
25. Couralet, C., Van den Bulcke, J., Ngoma, L. M., Van Acker, J. & Beeckman, H. Phenology in functional groups of Central African trees. *J. Trop. For. Sci.* **25**, 361–374 (2013).
26. Vico, G., Dralle, D., Feng, X., Thompson, S. & Manzoni, S. How competitive is drought deciduousness in tropical forests? A combined eco-hydrological and eco-evolutionary approach. *Environ. Res. Lett.* **12**, 65006 (2017).
27. Bennett, A. C., McDowell, N. G., Allen, C. D. & Anderson-Teixeira, K. J. Larger trees suffer most during drought in forests worldwide. *Nat. Plants* **1**, 15139 (2015).
28. *The Charcoal Transition: Greening the Charcoal Value Chain to Mitigate Climate Change And Improve Local Livelihoods* (FAO, 2017).
29. Lewis, S. L., Malhi, Y. & Phillips, O. L. Fingerprinting the impacts of global change on tropical forests. *Philos.T. Roy. Soc. B* **359**, 437–462 (2004).
30. *Rapport Annuel INEAC-Luki* (INEAC, 1947).
31. Coppieters, G. *Inventaris van het archief van de Rijksplantages en de Regie der Plantages van de Kolonie, het Nationaal Instituut voor de Landbouwkunde in Belgisch-Congo en de Documentatiedienst voor Tropische Landbouwkunde en Plattelandsontwikkeling 1901–1999* (REPCO, 2013).
32. *Biographie Coloniale Belge/Biographie Belge d'Outre-Mer* IX (Académie Royale des Sciences d'outre-mer, 2015).
33. *Rapport Annuel INEAC-Luki* (INEAC,1946).
34. *Rapport Annuel INEAC-Luki* (INEAC,1948).
35. De Mil, T., Vannoppen, A., Beeckman, H., Van Acker, J. & Van Den Bulcke, J. A field-to-desktop toolchain for X-ray CT densitometry enables tree ring analysis. *Ann. Bot.* **117**, 1187–1196 (2016).
36. Gärtner, H. & Nievergelt, D. The core-microtome: a new tool for surface preparation on cores and time series analysis of varying cell parameters. *Dendrochronologia* **28**, 85–92 (2010).
37. Dierick, M. et al. Recent micro-CT scanner developments at UGCT. *Nucl. Instrum. Meth. A* **324**, 35–40 (2014).
38. Vlassenbroeck, J. et al. Software tools for quantification of X-ray microtomography at the UGCT. *Nucl. Instrum. Meth. A* **580**, 442–445 (2007).
39. Worbes, M. in *Encyclopedia of Forest Sciences* Vol. 2 (eds. Burley, J., Evans, J. & Youngquist, J. A.) 586–599 (Academic Press, Cambridge, 2004).
40. Tarelkin, Y. et al. Growth-ring distinctness and boundary anatomy variability in tropical trees. *IAWA J.* **37**, 275–294 (2016).
41. Hietz, P. A simple program to measure and analyse tree rings using Excel, R and SigmaScan. *Dendrochronologia* **29**, 245–250 (2011).
42. Lopez-Gonzalez, G., Lewis, S. L., Burkitt, M. & Phillips, O. L. ForestPlots.net: a web application and research tool to manage and analyse tropical forest plot data. *J. Veg. Sci.* **22**, 610–613 (2011).
43. *R: A Language and Environment for Statistical Computing* (R Core Team, 2008).
44. Chave, J. et al. Improved allometric models to estimate the aboveground biomass of tropical trees. *Glob. Change Biol.* **20**, 3177–3190 (2014).
45. Feldpausch, T. R. et al. Tree height integrated into pantropical forest biomass estimates. *Biogeosciences* **9**, 3381–3403 (2012).
46. Lopez-Gonzalez, G., Sullivan, M. J. P. & Baker, T. R. BiomasaFP package. Tools for analysing data downloaded from ForestPlots.net. R package version 0.2.1 (ForestPlots/BiomasaFDP, 2015); http://www.forestplots.net/en/resources/analysis.
47. Aalde, H. et al. Forest Land. *IPCC Guidelines for National Greenhouse Gas Inventories* Vol. 4: Agriculture, Forestry and Other Land Use, Ch 4, 1–29 (IPCC, 2006).
48. Talbot, J. et al. Methods to estimate aboveground wood productivity from long-term forest inventory plots. *Forest Ecol. Manage.* **320**, 30–38 (2014).
49. Clark, D. A. et al. Measuring net primary production in forest concepts and field methods. *Ecol. Appl.* **11**, 356–370 (2001).
50. Benjamini, Y. & Hochberg, Y. Controlling the false discovery rate: a practical and powerful approach to multiple testing. *J. R. Stat. Soc. Ser. B* **57**, 289–300 (1995).

Acknowledgements

Nkulapark: W.H. and T.D.M. were both funded by the Brain programme of the Belgian Federal Government (BR/132/A1/AFRIFORD and BR/143/A3/HERBAXYLAREDD). The PhD project of T.D.M and the tenure track of J.V.d.B. were supported by Ghent University Special Research Fund (BOF). Fieldwork was sponsored by the King Leopold III fund for nature exploration and conservation. B.A.I. is supported by the Institut National pour l'Étude et la Recherche Agronomiques en R.D.Congo (INERA- RDC- Luki) and the École Régionale Postuniversitaire d'Aménagement et de Gestion intégrés des Forêts et Territoires tropicaux (ERAIFT Kinshasa). We thank WWF-RDC (G. Lejeune), INERA and ERAIFT for facilitating fieldwork in the Luki Reserve. We thank the INERA employees (J.-B. Ndunga, J.-M., F. Mbungu Phaka, L. Ngoma, P. Noble), the WWF ecoguards and the students of the Universities of Kinshasa (UNIKIN) and Boma for assistance in the field. For assistance with datasets we thank M. De Groot, K. Lievens, P. Dekeyser, S. Willen and J. Kempenaers. The 23 permanent inventory plots: This paper is also a product of the AfriTRON network, for which we are indebted to hundreds of institutions, field assistants and local communities for establishing and maintaining the plots. This network has been supported by the European Research Council (291585, 'T-FORCES' – Tropical Forests in the Changing Earth System, Advanced Grant to O.L.P. and S.L.L.), the Gordon and Betty Moore Foundation, the David and Lucile Packard Foundation, the European Union's Seventh Framework Programme (no. 283080, 'GEOCARBON') and Natural Environment Research Council (NERC) Consortium Grant 'TROBIT' (no. NE/D005590/1), 'BIO-RED' (no. NE/N012542/1) and a NERC New Investigators Grant, the Royal Society, the Centre for International Forestry (CIFOR) and Gabon's National Parks Agency (ANPN). We are indebted to the University of Yaounde I, the National Herbarium of Yaounde, Rougier-Gabon, the Marien Ngouabi University

of Brazzaville, WCS-Congo, Salonga National Park, WCS-D.R.Congo and the University of Kisangani for logistical support in Africa.

Author contributions

W.H., T.D.M., J.V.d.B., J.V.A. and H.B. conceived and designed the Nkulapark study and S.L.L. conceived the AfriTRON plot network. T.D.M. and B.A.I. coordinated collection of Nkulapark data and wood cores. T.D.M. and J.V.d.B. measured growth ring series. W.H. carried out the data analysis and wrote the paper. S.L.L., O.L.P., T.R.B. and Y.M. conceived the ForestPlots.net database, and most co-authors helped collecting AfriTRON forest census data. S.L.L., B.S., S.K.B., A.C.S., W.H., T.S., T.R.F., T.S., C.E.N.E. and L.W.W. coordinated forest plots data collection. M.J.P.S., G.L.G., S.L.L., O.L.P., T.R.B. and G.P. contributed tools to analyse and curate data. All co-authors commented on or approved the manuscript.

Competing interests

The authors declare no competing interests.

Additional information

Supplementary information is available for this paper at https://doi.org/10.1038/s41477-018-0316-5.

Reprints and permissions information is available at www.nature.com/reprints.

Correspondence and requests for materials should be addressed to W.H.

Publisher's note: Springer Nature remains neutral with regard to jurisdictional claims in published maps and institutional affiliations.

nature research

Corresponding author(s): Wannes Hubau (whubau@gmail.com)

Reporting Summary

Nature Research wishes to improve the reproducibility of the work that we publish. This form provides structure for consistency and transparency in reporting. For further information on Nature Research policies, see Authors & Referees and the Editorial Policy Checklist.

Statistical parameters

When statistical analyses are reported, confirm that the following items are present in the relevant location (e.g. figure legend, table legend, main text, or Methods section).

n/a	Confirmed	
☐	☒	The exact sample size (*n*) for each experimental group/condition, given as a discrete number and unit of measurement
☐	☒	An indication of whether measurements were taken from distinct samples or whether the same sample was measured repeatedly
☐	☒	The statistical test(s) used AND whether they are one- or two-sided *Only common tests should be described solely by name; describe more complex techniques in the Methods section.*
☐	☒	A description of all covariates tested
☐	☒	A description of any assumptions or corrections, such as tests of normality and adjustment for multiple comparisons
☐	☒	A full description of the statistics including central tendency (e.g. means) or other basic estimates (e.g. regression coefficient) AND variation (e.g. standard deviation) or associated estimates of uncertainty (e.g. confidence intervals)
☐	☒	For null hypothesis testing, the test statistic (e.g. *F*, *t*, *r*) with confidence intervals, effect sizes, degrees of freedom and *P* value noted *Give P values as exact values whenever suitable.*
☒	☐	For Bayesian analysis, information on the choice of priors and Markov chain Monte Carlo settings
☒	☐	For hierarchical and complex designs, identification of the appropriate level for tests and full reporting of outcomes
☒	☐	Estimates of effect sizes (e.g. Cohen's *d*, Pearson's *r*), indicating how they were calculated
☐	☒	Clearly defined error bars *State explicitly what error bars represent (e.g. SD, SE, CI)*

Our web collection on statistics for biologists may be useful.

Software and code

Policy information about availability of computer code

Data collection	Software used to visualize and measure growth-ring series (i.e. data collection): For each wood core, growth-ring series were visualized using two imaging methods as described by ref.36 : (i) first, density profiles were calculated from X-ray CT scans of entire wood cores, then (ii) the cores were surfaced with a core microtome37 and scanned using a flatbed scanner (EPSON Perfection 4990 PHOTO). To obtain X-ray CT volumes, cores were scanned at 110 µm resolution with the Nanowood CT facility from the Centre for X-ray Computed Tomography of Ghent University (UGCT, www.ugct.ugent.be)38, developed in collaboration with XRE (www.xre.be; now part of the TESCAN ORSAY HOLDING a.s.). Reconstruction was performed with the Octopus software package on a GeForce GPX 770 4GB GPU38,39.
Data analysis	1. Software used to analyze growth-ring series : X-ray and flatbed scans were analysed using the toolchain for tree-ring analysis described by De Mil et al. (ref. 36). This toolchain semi-automatically indicates the growth-ring boundaries and calculates growth-ring width series. Depending on the visibility of the growth-ring patterns, either the X-ray or the flatbed scans were used to check growth-ring boundaries and measure growth-ring widths. Growth-ring boundaries were distinguished using visual wood anatomical characteristics such as distended rays, flattened fibers and terminal parenchyma bands5,40,41. For unclear ring boundaries, microscopic thin sections were taken to study wood anatomy at high resolution using an Olympus BX60 microscope (Fig.1). Images of wood cores are available using the following link : https://figshare.com/s/e6101fe7d330f8ea140a . This folder also contains all annotation documents needed to visualize growth ring boundaries on the wood samples. The README document in the folder is a guideline to install and use the DHXCT toolbox published by De Mil et al. (ref.36).

2. Software and code used to analyse the permanent inventory plot data :
All selected plots are part of the African Tropical Rainforest Observatory Network (AfriTRON; www.afritron.org). These data are curated in the ForestPlots.net database43, and subject to identical quality control and quality assurance procedures. All calculations of plot data metrics described hereafter were performed using the R statistical platform44, version 3.2.1. Commands to calculate AGC-stock and AGC-sink are implemented in the BiomasaFP R package 47.The input data and R-scripts to generate the figures and tables are available for download using the following private link : https://figshare.com/s/06c793575d3b52ef5574.

For manuscripts utilizing custom algorithms or software that are central to the research but not yet described in published literature, software must be made available to editors/reviewers upon request. We strongly encourage code deposition in a community repository (e.g. GitHub). See the Nature Research guidelines for submitting code & software for further information.

Data

Policy information about availability of data

All manuscripts must include a data availability statement. This statement should provide the following information, where applicable:

- Accession codes, unique identifiers, or web links for publicly available datasets
- A list of figures that have associated raw data
- A description of any restrictions on data availability

1. Code and data availability statement (including links) :
The input data and R-scripts to generate the figures and tables are available for download using the following private link : https://figshare.com/s/06c793575d3b52ef5574. Images of wood cores are available using the following link : https://figshare.com/s/e6101fe7d330f8ea140a . This folder also contains all annotation documents needed to visualize growth ring boundaries on the wood samples (please consult the README document for guidelines). Wood samples used to conduct this analysis are stored in the Tervuren xylarium (http://www.africamuseum.be/collections/browsecollections/naturalsciences/earth/xylarium). These samples may be studied, within the Tervuren xylarium, upon request addressed to the curator H.B. (hans.beeckman@africamuseum.be) or the corresponding author W.H. (whubau@gmail.com).

2. List of figures with associated raw data :
Raw data for Fig.2 can be reproduced and checked using the images of wood cores available from figshare (cfr link above). Fig.2 can be reproduced from processed data using the input datafiles and script available on figshare (cfr link above).This script also produces Supplementary Figure 4.
The raw data and the script used to produce Fig.3 and Table 1 are available on figshare (cfr link above).

3. Restrictions on data availability :
All permanent inventory plot data is bound to data-use restrictions defined on Forestplots.net. To avoid unauthorized use of data, the input files on figshare provide only the information that is necessary to reproduce the figures and the tables using the r-scripts.

Field-specific reporting

Please select the best fit for your research. If you are not sure, read the appropriate sections before making your selection.

☐ Life sciences ☐ Behavioural & social sciences ☒ Ecological, evolutionary & environmental sciences

For a reference copy of the document with all sections, see nature.com/authors/policies/ReportingSummary-flat.pdf

Ecological, evolutionary & environmental sciences study design

All studies must disclose on these points even when the disclosure is negative.

Study description

Here, we take advantage of a remarkable rediscovery of a historic forest inventory plot to probe the age structure of mixed African rainforests in a way that hasn't been possible to date. The Nkulapark plot was established in 1948 in the southwest of the Democratic Republic of the Congo (Supplementary Fig.1). A total of 6315 trees (DBH>=5cm) were tagged and monitored weekly for 9 years, before the plot was abandoned in 1957. During a sampling campaign in 2014, we rediscovered 450 surviving tagged trees. Growth-ring series of 55 of these trees were measured on increment cores or stem discs (Supplementary Table 1). We accurately estimated total tree age and carbon age of these trees, using the grown-in iron nail as a timestamp. Discolorations and lumps caused by the nail exactly marked the year of tagging (1948) and demarcated the number of growth rings formed over a period of 66 years (1948-2014) (see Fig.1 for an example). This allowed to estimate the rate of growth-ring formation and infer total tree age for each individual tree (Fig.2).

We used the Crown Illumination Index of Dawkins & Field (hereafter referred to as CI Index or CII)(ref.21,22) to compare growth patterns and tree age among different rainforest strata in the rediscovered Nkulapark trees (Fig.2). The 5 different CII classes are illustrated in Fig.3a (ref.21). The first class (CII=1) contains understory trees receiving no direct light. The second class (CII=2) contains sub-canopy trees receiving only lateral light. The third class (CII=3) contains sub-canopy trees receiving some vertical light (10-90% of the vertical projection of the crown is exposed to vertical light). The fourth class (CII=4) contains canopy trees with a crown that is almost completely exposed to vertical light. The fifth class (CII=5) contains emergent trees with a crown that is completely exposed to vertical and lateral light in a 45 degree curve.

To test if our findings hold true in a wider geographic context, we compared growth and age patterns among the different forest strata in 23 Central African permanent forest plots with a similar mixed species composition as the Nkulapark (Fig.3, Table 1, Supplementary Fig.1 and Supplementary Table 2). These plots are demarcated rectangles or squares of median size 1 ha where each

tree is mapped, tagged and measured according to standard protocols (ref.1,2). Diameter at breast height (DBH) of each tree with DBH>= 10 cm was measured at least twice, with an average monitoring period of 9 years. Small trees that grew larger than 10cm during the monitoring period were recorded as recruits, tagged and mapped. Trees that died were carefully recorded. We used repeated diameter measurements to estimate the growth rate of each individual tree. We estimated total tree age by dividing the final diameter (mm) by the growth rate (mm yr-1). We estimated tree-level mean carbon age as the average age of each year ring, weighted by the carbon content of each year ring6, with a year ring sequence deduced from the growth rate (formula 1 in the Methods section). For each forest stratum within each plot, we calculated above-ground biomass-carbon (hereafter AGC) stock and AGC net change (sink) using standard methods (ref.1,2) (Table 1).

Research sample

1. Long-term growth records from the Nkulapark

1.1 original plot design and monitoring (1948-1957)
We rediscovered trees that were monitored within the Nkula experimental park. The Nkulapark is a phenology and tree growth monitoring plot covering 174 ha within the Luki Man and Biosphere reserve, located in the southern Mayumbe mountains in the Democratic Republic of the Congo (ref. 24) (Supplementary Fig.1). The Nkulapark was established in 1948. A total number of 6315 trees were tagged along 29.2 km of observation paths following the contour lines of the Nkula river valley (Supplementary Fig.1). Tree selection was performed by randomly selecting trees from the pool of trees > 5 cm dbh in 1948. As such the dataset contains a representative selection of trees in all diameter classes constituting the main carbon pool of the Nkulapark. From 1948 to 1957 yearly diameter measurements were performed on the 6315 tagged trees. Mortality events were recorded carefully in the datasheets. Trees were measured at a height of 1.3 m and the point of measurement (POM) was indicated on the tree with a horizontal line of lead-based paint. For trees with buttresses or deformities, the POM was raised to a point high enough to avoid the irregularities interfering with diameter measurements at subsequent censuses. For trees with extremely high buttresses, diameters were estimated. The experiment was abandoned in 1957 but the map and the datasheets were rediscovered and digitized in 2008 and 2014.

1.2 Rediscovery and monitoring of 450 trees in 2014
During a field campaign in august 2014, we aimed at rediscovering and remeasuring a maximum of the trees tagged in 1948, to establish a unique long-term growth dataset. Each of the original 6315 Nkulapark trees were labelled during the first census in 1948 with a zinc number tag that was attached to the tree using an iron nail of 8 cm long. A part of these trees were indicated on the original 1948 map. During a first prospective field campaign in 2014, this map was digitized and georeferenced with QGIS (QGIS development team, 2016) using landmarks such as easily rediscovered trees, contour lines and observation paths that were still visible and could be tracked with a Garmin 64s GPSmap (see Supplementary Fig.1). Based on this map, we pinpointed the approximate location of 1521 individuals that were recorded as alive in 1957. During a second field campaign in 2014, these 1521 individuals were searched for. 450 of them were found alive, 16 were found dead and the remaining 1057 could not be relocated and were assumed to be dead and rotten away, albeit some may have been missed. In-depth analysis of survivorship rates over the 1948-1957 period confirmed that the number of rediscovered trees is close to the expected number of survivors, although a substantial part of the understory trees may have been missed (Supplementary Fig.2). However, in-depth analysis showed that our dataset of 450 rediscovered trees is representative to compare growth and age patterns among the different forest strata in the Nkulapark area (Supplementary Fig.3, Supplementary Discussion). The original 1948 tree tags and nails of the rediscovered trees were either still present outside the trunk or detected inside the tree using a metal detector (BHJS, Bounty Hunter, USA). Scars on the trunk indicated the presence of an overgrown nail, and repelled number tags were sometimes found on or in the ground nearby the tree using the metal detector. In most cases, the numbers on the tags were still readable. On 95% of the rediscovered trees, the Lead-based paint of the POM was still visible, allowing a representative DBH measurement.

2. Plot inventory data
To test if our findings hold true in a wider geographic context, we estimated mean tree age and carbon age of the different forest strata in 23 Central African permanent forest plots located in four different Central African countries (Cameroon, Gabon, Congo Brazzaville, D.R.Congo) (Supplementary Fig.1 and Supplementary Table 2). Plots were selected if at least 65% of the trees belonged to species that also occur in the Nkulapark. Furthermore, plots selected for analysis conformed to the following criteria1,2,42: (1) plots had an actual plot area of ≥0.2 ha, (2) plots were georeferenced, (3) all trees with DBH ≥100 mm were measured, (4) the majority of stems were identified to species level, (5) plots had at least 2 censuses, (6) plots had a total monitoring length of ≥ 3 years, (7) plots were situated within structurally intact, apparently mature forest (excluding young or open forests), (8) plots were free from major human impacts, (9) plots were located at ≥50m from the anthropogenic forest edge, (10) altitude was below 1500 m.a.s.l., (11) mean annual air temperature was ≥20.0°C, (12) mean annual precipitation was ≥1000 mm yr-1, (13) plots were located in terra firme forest. For analysis purposes, plots smaller than 0.5 ha that were within 1 km of each other and located in similar forest types were merged (i.e. the LME cluster). All selected plots are part of the African Tropical Rainforest Observatory Network (AfriTRON; www.afritron.org). These data are curated in the ForestPlots.net database43, and subject to identical quality control and quality assurance procedures. All calculations of plot data metrics described hereafter were performed using the R statistical platform44, version 3.2.1.

Sampling strategy

Wood samples for growth-ring analysis were taken from rediscovered trees if following criteria were met : (a) the nail was still present in the wood, either totally grown-in or partly sticking out of the trunk, (b) the exact position of the nail could be identified visually or with the metal detector, (c) the nail was not overgrown by excessive wound tissue, buttresses or other deformities. As such, increment cores or stem disks were taken near the nail for 58 of the rediscovered trees. For each sampled tree, increment cores were taken a few centimetres above, below, to the left and to the right of the nail using a 40cm Pressler bore. For each tree, two additional cores were taken at 120° from the nail trace along the circumference of the tree. As such, 6 core samples were available for each tree. This maximised the chance of sampling the pith of the tree. In order to study and describe the reaction of the wood after tagging, additional larger wood samples containing the nail were extracted from 30 trees using a saw and a chisel.

Data collection

The Nkulapark was established and managed by the Institut National pour l'Etude Agronomique du Congo Belge (INEAC), which was later renamed Institut National pour l'Etude et la Recherche Agronomique en R.D.Congo (INERA, http://www.inera-drc.org). The person in charge of the tagging and the measurements was Léon Toussaint, who worked as a botanist in the Luki reserve between 1946 and 195233. The planning of the plot was first announced in the INEAC-Luki annual report of 194634. A total of 29.2 km of observation paths were cut in the forest in 1947, following the contour lines of the Nkula river valley (Supplementary Fig.1)31. A total

number of 6315 trees were tagged by the end of 194731, so we assume that first wood formation after tagging occurred during the wet season that started in October 1948. First diameter measurements were performed in 1948 (ref.33).

Map digitization, rediscovery of trees in the field and sampling wood cores was performed by Tom De Mil and Bhély Angoboy in 2014. Digitization was performed using a Garmin 64s GPSmap. Rediscovering tags and nails was done using a metal detector (BHJS, Bounty Hunter, USA). Cores were taken using a Pressler core borer.

Visualizing and measuring growth-ring series was performed by Tom De Mil. For each wood core, growth-ring series were visualized using two imaging methods as described by ref.36 : (i) first, density profiles were calculated from X-ray CT scans of entire wood cores, then (ii) the cores were surfaced with a core microtome (ref. 37) and scanned using a flatbed scanner (EPSON Perfection 4990 PHOTO). To obtain X-ray CT volumes, cores were scanned at 110 µm resolution with the NanowWood CT facility from the Centre for X-ray Computed Tomography of Ghent University (UGCT, www.ugct.ugent.be)38, developed in collaboration with XRE (www.xre.be; now part of the TESCAN ORSAY HOLDING a.s.). Reconstruction was performed with the Octopus software package on a GeForce GPX 770 4GB GPU38,39. X-Ray ray and flatbed scans were analysed using the toolchain for tree-ring analysis described by De Mil et al. (ref. 36). This toolchain semi-automatically indicates the growth-ring boundaries and calculates growth-ring width series. Depending on the visibility of the growth-ring patterns, either the X-Ray ray or the flatbed scans were used to check growth-ring boundaries and measure growth-ring widths. Growth-ring boundaries were distinguished using visual wood anatomical characteristics such as distended rays, flattened fibers and terminal parenchyma bands5,40,41. For unclear ring boundaries, microscopic thin sections were taken to study wood anatomy at high resolution using an Olympus BX60 microscope (Fig.1).

Forestplots inventory data were recorded using standard procedures described by ref. 1,2. Principal Investigators and field leaders for each inventory plot are specified in Supplementary Table 2.These plots are demarcated rectangles or squares of at least 0.2ha where each tree is mapped, tagged and measured according to standard protocols (ref. 1,2,42). Diameter at breast height (DBH) of each tree with DBH>= 10 cm was measured at least twice, with a minimum total monitoring period between the first and the last census of at least 3 years (Supplementary Table 2). Small trees that grew larger than 10cm during the monitoring period were recorded as recruits, tagged and mapped. For trees that died, the mechanism of mortality was recorded carefully during the census at which the tree was found dead. Dead trees were no longer measured or monitored afterwards.

Timing and spatial scale

1. Timing
Tagging and initial measurement of all Nkulapark trees was performed before and during the dry season of 1948 (january-august). Hence, the first wood formed after the nail mark represents the growing season from october 1948 till february 1949. All Nkulapark trees were measured yearly between 1948 and 1957 (except in 1955). Rediscovery, remeasurement and sampling of Nkulapark trees was performed in june-august 2014.
The monitoring period of the 23 permanent forest plots used for the main analysis varied per cluster. The start of the monitoring period varied between 1993 and 2009, while the end of the monitoring period varied between 2013 and 2017. Total monitoring length varied between 5 and 19.9 years (Supplementary Table 2).

2. Spatial scale
The Nkulapark plot covers 174 ha within the Luki Man and Biosphere reserve, located in the southern Mayumbe mountains in the Democratic Republic of the Congo (Supplementary Fig.1).
To test if our findings hold true in a wider geographic context, we estimated mean tree age and carbon age of the different forest strata in 23 Central African permanent forest plots located in four different Central African countries (Supplementary Fig.1 and Supplementary Table 2). Plots have a median size of 1 ha.

Data exclusions

Three (out of 58) measured growth-ring series were not used for analysis because estimated missing core length of each core exceeded 20 cm. As such, growth-ring series of 55 trees were retained (Supplementary Table 1).
23 of the selected permanent forest inventory plots were used for the main analysis because CII was recorded. An additional 27 plots were used for Supplementary analysis (Supplementary Table 4).

Reproducibility

The input data and R-scripts to generate the figures and tables are available for download using the following private link : https://figshare.com/s/06c793575d3b52ef5574. Images of wood cores are available using the following link : https://figshare.com/s/e6101fe7d330f8ea140a . This folder also contains all annotation documents needed to visualize growth ring boundaries on the wood samples (please consult the README document for guidelines). Wood samples used to conduct this analysis are stored in the Tervuren xylarium (http://www.africamuseum.be/collections/browsecollections/naturalsciences/earth/xylarium). These samples may be studied, within the Tervuren xylarium, upon request addressed to the curator H.B. (hans.beeckman@africamuseum.be) or the corresponding author W.H. (whubau@gmail.com).

Randomization

To distinguish between understory, sub-canopy, canopy and emergent trees in the Nkulapark and the permanent forest plots, we use the Crown Illumination Index (CII) of Dawkins & Field (ref. 21 and 22). The Crown Illumination Index (CII) distinguishes 5 classes. The first class (CII=1) contains understory trees receiving no direct light (crown is not lit directly vertically or laterally). The second class (CII=2) contains trees in the understory receiving only lateral light. The third class (CII=3) contains intermediate trees receiving some vertical light (10-90% of the vertical projection of the crown is exposed to vertical light). The fourth class (CII=4) contains canopy trees with a crown that is almost completely exposed to vertical light (90-100% of the vertical projection of the crown is exposed to vertical light). The fifth class (CII=5) contains emergent canopy trees with a crown that is completely exposed to vertical and lateral light in a 45 degree curve. Fig.3 illustrates the 5 classes with a drawing modified from ref.21. The Crown Illumination Index was recorded in 23 of the selected permanent inventory plots. In each plot where the index was recorded, each tree was attributed to one of the CII classes. The index was attributed in the field, mostly during one census and mostly by a single person.

We estimated mean tree age, mean carbon age, mean AGC-stock and mean AGC-sink for each of the CII classes in each plot where the index was recorded. None of the metrics reported in Table 1 meet the criterion of homogeneity of variances (Bartlett test). Therefore, differences among the CII classes were tested using the non-parametric Dunn's rank-sum test. To avoid the multiple comparison problem, we used the Benjamini-Hochberg p-value adjustment (ref.30) ('dunn.test' package in R, ref.44).

Blinding

Blinding was not relevant to our study. Selection of rediscovered Nkulapark trees and selection of permanent forest inventory plots were based on strict criteria described above.

Did the study involve field work? ☒ Yes ☐ No

Field work, collection and transport

Field conditions

The Nkulapark is located in the Mayumbe hills, which experience a humid tropical climate with a dry season between mid-May and mid-October and a short dry season from mid-December to mid-February. Yearly precipitation ranges from 649 mm to 1853 mm with a mean precipitation of 1173 mm. Temperature ranges between 19 °C and 30 °C with a mean temperature of 25.5 °C (ref.24).

Location

The Nkula park was set up as a permanent monitoring plot covering 174 ha within the Luki Man and Biosphere reserve, located in the southern Mayumbe mountains in the Democratic Republic of the Congo (Supplementary Fig.1). Latitude ranges between -5.605 and -5.630 ; longitude ranges between 13.098 and 13.107 ; altitude ranges between 140 and 370 meter above sea level.

Access and import/export

Research was conducted in close collaboration with INERA (Institut National pour l'Etude et la Recherche Agronomique en R.D.Congo, http://www.inera-drc.org). A 'Termes de References' was prepared and signed by the field leaders (T.D.M and B.A.I.) and the director of the INERA station in the Luki reserve (Jean-Baptiste Ndunga). Fieldwork was carried out with the assistance of INERA employees (Jean-Maron Maloti Ma Songo, Fils Mbungu Phaka, Leonard Ngoma, Jean-Baptiste Ndunga, Noble, Plaside). Some of these employees were trained as ecoguards by WWF. An official export permit for wood samples was issued by INERA-Luki.

Disturbance

Fieldwork was carried out within the UNESCO 'Man and the Biosphere reserve (MAB)' of Luki (ref.24). MAB reserves consist of an integrally protected 'Central Zone', a 'Transition Zone' and a 'Buffer Zone'. The Nkula experimental park is located in the Transition Zone, which is designated for local activities (e.g. extensive farming) and scientific research.

Wood cores were taken from 58 trees. Extraction of these cores leave a cylindrical hole in the tree with a diameter of 0.5 cm. Extracting cores wounds the tree, but trees have a coordinated system to limit the damage from small wounds. This system is called compartmentalization (for more information, see Shigo, A.L. 1984. Compartmentalization: a conceptual framework for understanding how trees grow and defend themselves. Annual Review of Phytopathology 22, 189-214). Trees growing in natural tropical forests are subject to a wide range of wounding events such as branch breakages due to storms or bark damage by e.g. elephants. If the damage is not too intense, trees are able to successfully compartmentalise this damage and usually continue growing. According to Shigo (1984), the process of compartmentalisation explains "the very longevity and capacity of perennial plants to survive countless wounds and subsequent development of even more countless pathogenic and parasitic microorganisms". Our extraction of increment cores from trees has been an additional, although very minor, form of wounding.

Furthermore, we extracted additional larger wood samples from 30 of the sampled trees, using a saw and a chisel. These wounds will likely affect these trees in a more severe way than the wood cores. We expect some of these trees to die, but others will probably recover due to their ability to compartmentalise. Finally, we note that 1 very small tree was entirely cut to extract a stem disk containing the nail.

We conclude that our sampling affected a very small percentage of the trees within the 174 ha Nkulapark, while most of the sampled trees will not suffer permanent damage from the sampling.

Reporting for specific materials, systems and methods

Materials & experimental systems

n/a	Involved in the study
☐	☒ Unique biological materials
☒	☐ Antibodies
☒	☐ Eukaryotic cell lines
☒	☐ Palaeontology
☒	☐ Animals and other organisms
☒	☐ Human research participants

Methods

n/a	Involved in the study
☒	☐ ChIP-seq
☒	☐ Flow cytometry
☒	☐ MRI-based neuroimaging

Unique biological materials

Policy information about availability of materials

Obtaining unique materials

Wood samples used to conduct this analysis are stored in the Tervuren xylarium. Metadata and images of these samples will be available from http://www.africamuseum.be/collections/browsecollections/naturalsciences/earth/xylarium. These samples may be studied, within the Tervuren xylarium, upon request addressed to the curator H.B. (hans.beeckman@africamuseum.be) or the corresponding author W.H. (whubau@gmail.com).